PHYSICAL REVIEW C **84**, 022801(R) (2011)

Direct total cross section measurement of the $^{16}O(\alpha,\gamma)^{20}Ne$ reaction at $E_{c.m.} = 2.26$ MeV

U. Hager,[1,*] J. R. Brown,[2] L. Buchmann,[3] M. Carmona-Gallardo,[4] L. Erikson,[5] J. Fallis,[3] U. Greife,[1] D. Hutcheon,[3] D. Ottewell,[3] C. Ruiz,[3] S. Sjue,[3,†] and C. Vockenhuber[6]

[1]*Colorado School of Mines, Golden, Colorado, USA*
[2]*Department of Physics, University of York, York, YO10 5DD, United Kingdom*
[3]*TRIUMF, Vancouver, Canada V6T 2A3*
[4]*Instituto de Estructura de la Materia, CSIC E-28006 Madrid, Spain*
[5]*Pacific Northwest National Laboratory, Richland, WA, USA*
[6]*ETH Zurich, Zurich, Switzerland*

(Received 17 June 2011; published 23 August 2011)

In stellar helium burning, ^{16}O represents the endpoint of the helium-burning sequence due to the low rate of $^{16}O(\alpha,\gamma)^{20}Ne$. We present a new direct measurement of the total capture reaction rate of $^{16}O(\alpha,\gamma)^{20}Ne$ at $E_{c.m.} = 2.26$ MeV employing the DRAGON recoil separator. For the first time, the total S factor and its contributing direct capture transitions could be determined in one experiment.

DOI: 10.1103/PhysRevC.84.022801 PACS number(s): 26.20.Fj, 98.80.Ft, 97.10.Cv

The first reaction of the stellar helium-burning stage is the triple-α process, which produces ^{12}C. After the production of ^{12}C, other α-cluster nuclei can, in principle, be produced. At typical helium-burning temperatures of 1–3 $\times$ 10^8 K (effective energy for helium-burning reactions, $E_{c.m.} \approx 0.3$ MeV), their production is, however, hindered by the increasing Coulomb barriers [1]. Thus, two of the main end products of steady-state helium burning are ^{12}C and ^{16}O, with their ratio determined in part by the $^{16}O(\alpha,\gamma)^{20}Ne$ rate. This ratio also determines the abundances of the products of later carbon burning, mainly ^{20}Ne, ^{23}Na, $^{23,24}Mg$, and ^{28}Si, compared to the products of oxygen burning, like aluminium [1].

The reason for the low $^{16}O(\alpha,\gamma)^{20}Ne$ rate at helium-burning temperatures is the absence of an excited state in ^{20}Ne in the relevant energy region (see Fig. 1); the 2^- state is of unnatural parity and therefore cannot be populated by this reaction. At stellar energies, the reaction will thus only proceed via nonresonant direct capture (DC), either into the ground state or through the first excited state at 1.6 MeV.

Several studies of the $^{16}O(\alpha,\gamma)^{20}Ne$ DC have been conducted, both theoretically and experimentally. Langanke [2] calculated the $^{16}O(\alpha,\gamma)^{20}Ne$ DC cross section using a semimicroscopic OCM (orthogonality condition model) calculation. In the energy range $E_{c.m.} \approx 0.4$–2 MeV they predicted the S factor to be approximately linear in energy, $S_{DC} = 1.88\,\text{MeV b} + 1.05\,\text{b} \cdot E$, or $S_{DC} = 4.3$ MeV b at $E_{c.m.} = 2.3$ MeV. Hahn *et al.* [3] measured the reaction in inverse kinematics with an ^{16}O beam on a windowless gas target, choosing energies sufficiently far from resonances in ^{20}Ne for DC to dominate. They measured the S factor for capture to the ground state as $S_0 = 0.26 \pm 0.07$ MeV b for $E_{c.m.} = 1.7$–2.35 MeV and calculated upper limits for the total nonresonant S factor of $S_{DC} = 2.8$ MeV b at $E_{c.m.} = 2.3$ MeV. For the astrophysically interesting energy $E_{c.m.} \approx 300$ keV, the total S factor is estimated using theoretical predictions for the branching ratios and energy dependence. The result is $S_{DC} = 0.7 \pm 0.3$ MeV b. Commenting on Ref. [3], Baye and Descouvemont [4] state that the calculated S factor is probably too low. They suggest the results obtained in Ref. [3] at $E_{c.m.} = 2.3$ and 2.35 MeV should be remeasured, and the recommended S factor should be multiplied at least by a factor of 2. Knee [5] measured the reaction cross section using HPGe detectors for the prompt γ's in normal kinematics using a windowless gas target. The DC was measured in the range $E_{c.m.} = 1.2$–2.32 MeV. For DC into the ground state an upper limit of $S_0 \leqslant 0.92$ MeV b was found, and for DC into the first excited state an upper limit of $S_2 \leqslant 2.45$ MeV b was found. The total nonresonant S factor is given as $S_{DC} \leqslant 3.37$ MeV b.

Most recently, Costantini *et al.* [6] presented an R-matrix analysis using previously unpublished data on capture to the first excited state. They assume the decay through the first excited state to contribute $S_2 = 75(10)\%S_{DC}$ at the astrophysically relevant $E_{c.m.} = 0.3$ MeV, and they give a total S factor at that energy of $S_{DC} = 1.9$ MeV b. From Fig. 14 of Ref. [6], the total S factor at $E_{c.m.} = 2.3$ MeV is $S_{DC} \approx 1.7$ MeV b.

Due to the low DC cross section and the relatively low efficiency of germanium detectors at high energies, most previous measurements of the DC contribution determined only the S_2 capture component through the first excited state in ^{20}Ne, with the S_0 component to the ground state derived from theory. On the other hand, Ref. [3] measured only the S_0 component. In this work, we present a measurement of the total DC rate at $E_{c.m.} = 2.26$ MeV measured at the DRAGON recoil separator [7], located at the ISAC facility at TRIUMF, Vancouver, Canada. A schematic view of the DRAGON facility is shown in Fig. 2. This specific beam energy was chosen as it is sufficiently far from the tails of the higher $J^\pi = 3^-$ and the lower 0^+ resonances for the DC to dominate the reaction. On the other hand, the reaction rate at this energy is still high enough to ensure adequate statistics for determining the branching ratio. An additional measurement was taken closer to the 3^- resonance

*uhager@mines.edu
†Present address: LANL, USA.

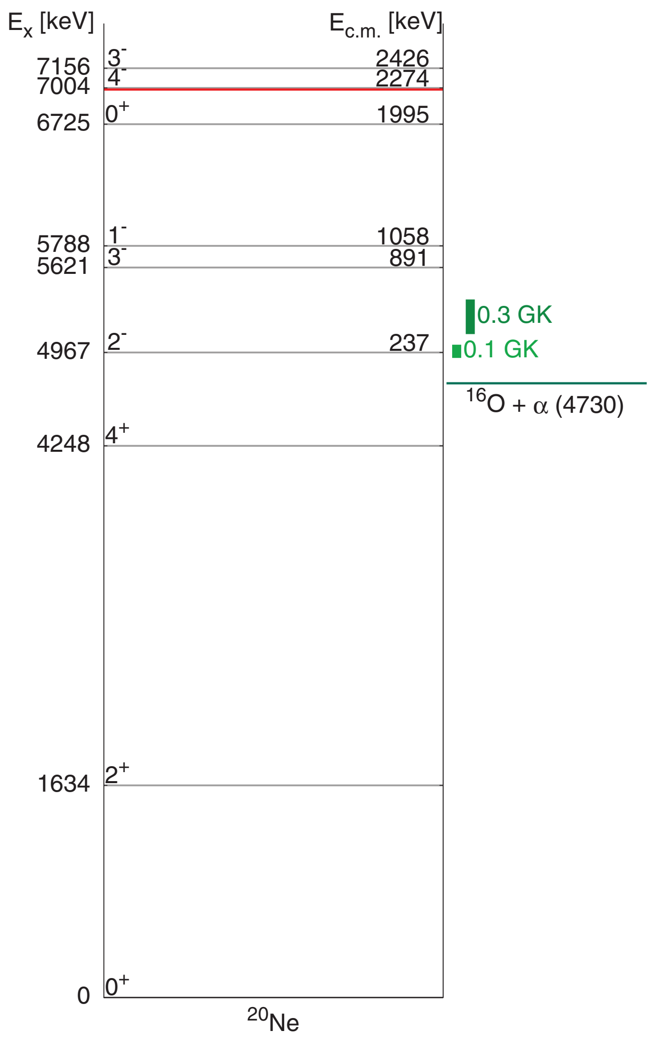

FIG. 1. (Color online) Excitation levels in ^{20}Ne. On the right-hand side, Gamow windows corresponding to 0.1 and 0.3 GK are indicated. The red line (second from the top) indicates the energy discussed in the present work.

to confirm that no resonant contributions remain at this energy.

The ^{16}O beam was produced by the Supernanogan off-line ion source [8] and accelerated to 715(1) keV/u. On average, the beam intensity at the DRAGON target was 9×10^{11} s^{-1}. The DRAGON windowless gas target was filled with ^{4}He maintained at a pressure within 3% of 8 Torr. The beam energy at the target exit was 698 keV/u; the energy range covered by the target was thus 2.24–2.29 MeV (center of mass). The DRAGON target is surrounded by an array of 30 BGO (Bismuth Germanate) γ detectors in a tight geometry, which were calibrated using the 6.13-MeV γ ray emitted by a ^{244}Cm-^{13}C source. To suppress background, the ^{20}Ne ions produced in the reaction were detected in coincidence with γ events in the BGO array, after separation from the beam using a two-stage electromagnetic separator with an acceptance of 21 mrad; the maximum cone angle of the ^{16}O$(\alpha,\gamma)^{20}$Ne reaction was 12 mrad. At the focal plane, an ionization chamber [9] was used to detect ^{20}Ne recoils from the reaction.

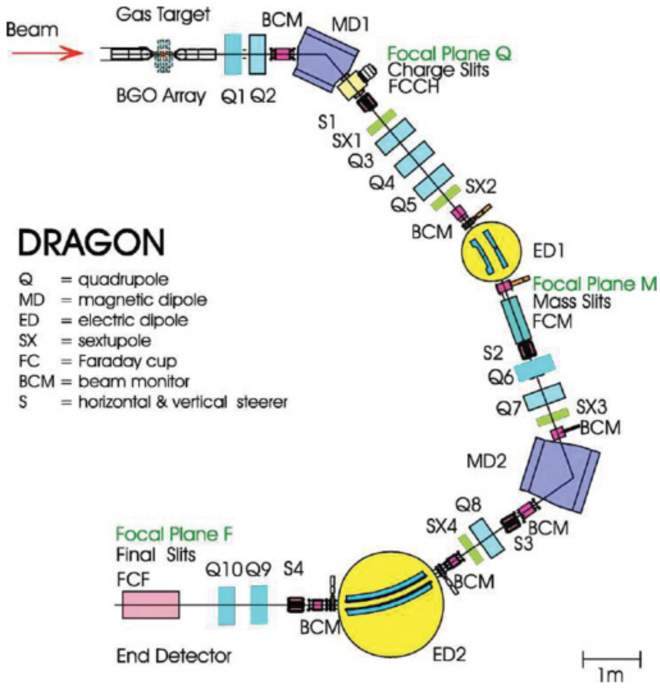

FIG. 2. (Color online) Schematic view of the DRAGON facility.

Its segmented anode enables stopping power measurement and thus particle identification (PID). Figure 3 gives an example of a PID plot, showing the energy (arbitrary units) deposited in the second anode versus the energy deposited in the first anode. The red circles represent all events detected in the ionization chamber, the blue crosses indicate a coincident γ detection in the BGO array, and the green line represents a gate on the data to identify the recoils and eliminate a "leaky" ^{16}O beam. As an additional PID parameter, the time of flight through the separator was used to identify valid recoil coincidence events. A total of 367 ^{20}Ne reaction recoils could thus be identified.

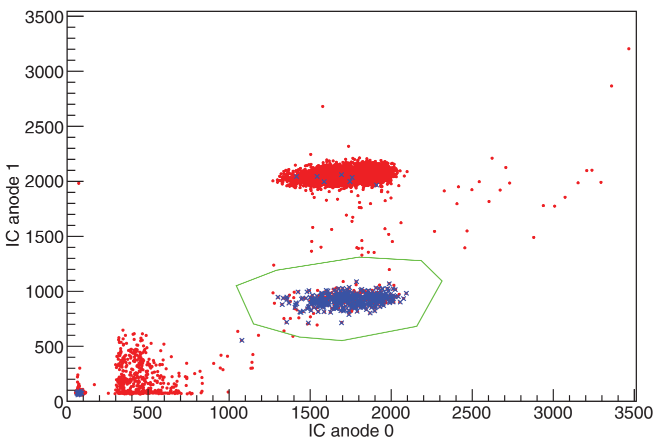

FIG. 3. (Color online) Ionization chamber PID: energy deposited in anode 1 vs energy deposited in anode 0 (given in arbitrary units). The red circles are recoils detected in the ionization chamber, the blue crosses are recoils in the ionization chamber coincident with a γ detection at the target, and the green line represents a software gate used to identify recoil events.

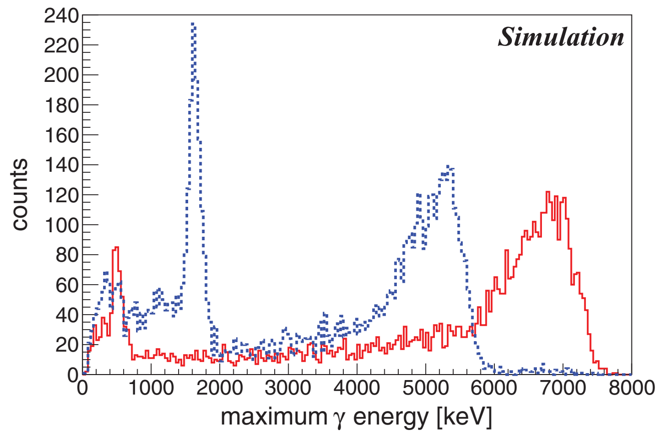

FIG. 4. (Color online) Simulation of pure S_0 (red solid line) and S_2 (blue dashed line). Shown is the maximum detected γ energy.

To determine the beam intensity, regular Faraday cup readings were taken, and, following the procedure outlined in Ref. [10], the total number of ^{16}O nuclei on target was determined to be $(181 \pm 3) \times 10^{15}$. Because the separator only transmits ^{20}Ne recoils of one charge state, determining the total cross section requires knowledge of the distribution of charge states of neon passing through helium. This distribution was measured using a beam of ^{20}Ne, also from the Supernanogan. The reaction measurements were conducted in charge state 4^+, which has a measured charge state fraction of 25(3)%. When using higher charge states, a decrease in beam suppression of the separator was observed, due to the ^{16}O beam in a lower charge state being transmitted to the focal plane.

Since both the separator transmission and the efficiency of the BGO array depended on the number of γ rays emitted in the reaction, the ratio of S_2/S_0 had to be determined. To this end, GEANT3 simulations were conducted assuming either pure S_0 or pure S_2 transitions; the resulting γ-ray spectra are shown in Fig. 4. The small number of counts in the S_2 simulation at 7 MeV indicates that accidental summing due to both γ's hitting the same BGO is very rare and is accounted for in the

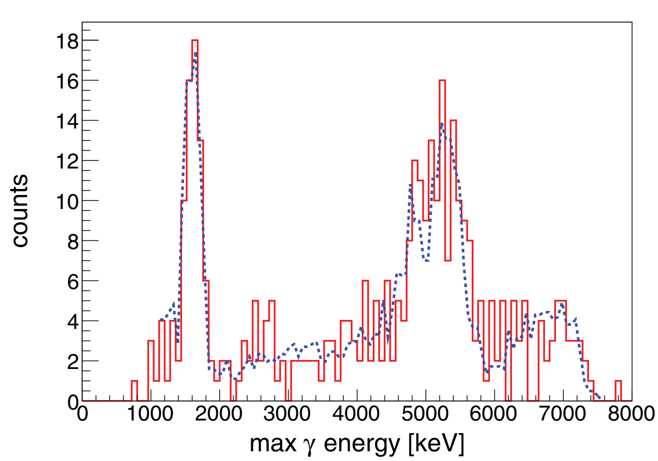

FIG. 5. (Color online) Maximum detected γ energy: solid line, measured; dashed line, simulation.

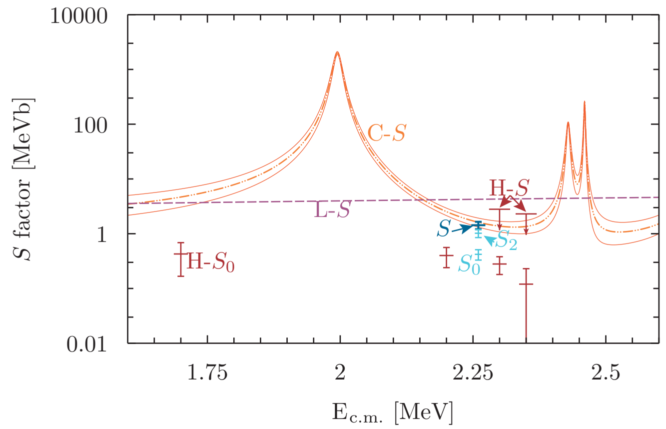

FIG. 6. (Color online) Comparison of this work to previous results: The orange dashed-dotted line denoted "C-S" is the total S factor given in Ref. [6], and the purple dashed line marked "L-S" is the total S factor from Ref. [2]. The red data points and upper limits are S_0 and S, respectively, taken from Ref. [3]. The blue data points are the results presented here.

simulation. The BGO detection efficiency for S_0 transitions was 60(2)% and for S_2 it was 75(2)%. The resulting simulated γ spectra were fitted to the measured one. Figure 5 shows the maximum γ energy detected for each valid recoil event (red solid line) together with the fitted simulation (blue dashed line). Note that energies deposited in neighboring detectors were not summed. The same procedure was applied using such addback spectra to account for energy lost to escape electrons, and both methods were found to agree within uncertainties. The S_2 contribution to the S factor was found to be 71(4)%. Using this value, the total efficiency of the DRAGON measurement could be determined, and the S factor was calculated to be $S = 1.43 \pm 0.22$ MeV b. From this absolute value and the ratio of S_0 to S_2 the two contributions were calculated to be $S_0 = 0.42 \pm 0.09$ MeV b and $S_2 = 1.02 \pm 0.17$ MeV b. This S_0 contribution agrees well with the results shown in Fig. 7 of Ref. [3] for $E_{c.m.} = 2.2$ MeV and $E_{c.m.} = 2.3$ MeV, but is larger than the weighted average including lower and higher energy values derived therein. This average is largely determined by the value measured at $E_{c.m.} = 2.35$ MeV; see the red data points in Fig. 6. As stated above, Baye and Descouvemont [4] recommended that S_0 at this energy be remeasured.

The total measured S factor is slightly lower than the one calculated in Ref. [6], though still within the uncertainties shown in Fig. 14 of Ref. [6]. A comparison of the S factor derived in this work and previous literature values is shown in Fig. 6.

In conclusion, the results presented in this work represent the first direct measurement of the total S factor and its components of the DC cross section of the nuclear reaction ^{16}O(α,γ)^{20}Ne. It thus provides an important constraint for theoretical calculations aiming to extrapolate the S factor to the astrophysically relevant energy ranges. Further experiments and data analysis at lower energies are ongoing in order to facilitate such extrapolations; the results will be published at a later date.

We would like to thank the beam delivery and ISAC operations groups at TRIUMF. The authors gratefully acknowledge funding from the Natural Sciences and Engineering Research Council of Canada and the US DOE Office of Nuclear Physics. We also gratefully acknowledge the invaluable assistance in beam production from K. Jayamanna.

[1] C. E. Rolfs and W. S. Rodney, *Cauldrons in the Cosmos* (The University of Chicago Press, Chicago, 1988).
[2] K. Langanke, Z. Phys. **317**, 325 (1984).
[3] K. H. Hahn, K. H. Chang, T. R. Donoghue, and B. W. Filippone, Phys. Rev. C **36**, 892 (1987).
[4] D. Baye and P. Descouvemont, Phys. Rev. C **38**, 2463 (1988).
[5] H. Knee, Ph.D. thesis, Universität Stuttgart, 1994.
[6] H. Costantini *et al.*, Phys. Rev. C **82**, 035802 (2010).
[7] D. A. Hutcheon *et al.*, Nucl. Instrum. Methods A **498**, 190 (2003).
[8] K. Jayamanna, Rev. Sci. Instrum. **81**, 02A331 (2010).
[9] C. Vockenhuber, L. Buchmann, J. Caggiano, A. A. Chen, J. M. D'Auria, C. A. Davis, U. Greife, A. Hussein, D. A. Hutcheon, D. Ottewell, C. O. Ouellet, A. Parikh, J. Pearson, C. Ruiz, G. Ruprecht, M. Trinczek, and J. Zylberberg, Nucl. Instrum. Methods B **266**, 4167 (2008).
[10] J. M. D'Auria *et al.*, Phys. Rev. C **69**, 065803 (2004).